Shinq-Jen Wu, et.al. International Journal of Engineering Research and Applications
www.ijera.com
ISSN: 2248-9622, Vol. 15, Issue 9, September 2025, pp 59-78

RESEARCH ARTICLE OPEN ACCESS

Visualizing the Challenge: Decoding Sloppiness and Operating Principles in S-type Biological systems

Shinq-Jen Wu [1,*] andSing-Yu Lu [2]

[1,2] *Department of Electrical Engineering Da-Yeh University, 168 University Rd., Dacun Changhua 51591, Taiwan, R.O.C*

Abstract

The quantitative study of biological systems relies on three fundamental pillars—modeling, analysis, and control—to transform complex dynamics into actionable insights. While S-system models offer a powerful framework for representing biochemical interactions, two critical challenges hinder their practical application: pervasive parameter sloppiness (where vastly different kinetic parameters yield similar behaviors) and the lack of systematic methods to derive operating principles (rules governing biological controllability). Traditional analytical approaches struggle to address these issues due to the high-dimensional, nonlinear nature of S-systems.In this work, we present an integrated visualization-driven approach to decode sloppiness and extract operating principles from S-system models. Leveraging computational tools in the Simulink environment, we construct Hessian matrices to quantify hierarchical parameter sensitivity and reveal sloppiness spectra in S-system dynamics, develop control-theoretic methods to identify biologically interpretable design rules, and implement interactive visual analytics to bridge theoretical models with experimental feasibility.Our results demonstrate how visualization not only clarifies the geometric structure of sloppy parameter manifolds but also facilitates the discovery of robust control strategies. By combining these advances with our recently developed intelligent technologies for cancer classification and genetic network identification, we provide a practical framework for applying S-system theory to real-world biological challenges. This work establishes visualization as a discovery tool—transforming S-system complexities into interpretable design principles for synthetic biology and precision medicine.

Keywords: Fuzzy logic control, systems biology, computational biology, computational analysis, computational biology, graphical models

---

Date of Submission: 25-08-2025 Date of acceptance: 03-09-2025

I. INTRODUCTION

The inherent complexity of biological systems has long driven the development of mathematical frameworks to capture their nonlinear dynamics. From a quantitative perspective, addressing these challenges requires three fundamental pillars: modeling, analysis, and control. This framework involves selecting appropriate system representations to identify structural topologies and kinetic parameters, performing rigorous analyses to characterize system properties, and developing control strategies to steer systems toward desired targets.While Bartocci and Lió [1] argue that ODE-based models sufficiently capture biological behavior, and Voit [2] provides comprehensive reviews of biochemical systems theory applications, practical challenges persist. Sriyudthsak et al. [3] note that among various approaches, S-systems and Michaelis-Menten systems remain most promising for reconstructing gene networks in diseases and cancer.

S-system formalism—with its power-law representation of biochemical interactions—has proven uniquely capable of balancing mechanistic fidelity with analytical tractability [4, 5]. These systems, described by the differential equation:

$$\dot{x}_i = f^i = v_i^+ - v_i^- = \alpha_i \prod_{j=1}^{n+m} x_j^{g_{ij}} - \beta_i \prod_{j=1}^{n+m} x_j^{h_{ij}}, i = 1, \dots n \qquad (1)$$

where$\alpha_i$and β_i are the rate constants. The $g_{ij}$and h_{ij} denote net interactive strengths from x_j on x_i, offer remarkable versatility in representing biochemical interactions. The $x_i, i = 1, \dots n$ are dependent variables and $x_{n+1}, \dots x_{n+m}$ are independent variables, the values of which remains

constant during a period of an experiment.The modeling of S-systems constitutes a multi-objective, constrained optimization problem.Unlike Michaelis-Menten systems that follow bottom-up modeling through iterative experimentation, S-systems employ a top-down approach with parameters estimated through computational methods, making them particularly suitable for large-scale systems [6-9].These challenges of S-system modelling are particularly pronounced because in medium-to-large systems, kinetic constants represent relative strength rather than absolute interaction values. Traditional approaches often restrict parameter ranges unnecessarily (e.g., $(\alpha, \beta) \in [0,20], (g_{ij}, h_{ij}) = [-3,3]$) [10]) and struggle with high-dimensional systems [11-13]. Our previous work has developed various computational intelligence techniques—including fuzzy inference-based optimization [14], enhanced evolutionary algorithms [14-17], and novel cockroach swarm evolution [18]—to expand parameter ranges to$(\alpha, \beta) \in [0,100], (g_{ij}, h_{ij}) = [-100,100]$) and successfully achieve 30-gene S-system identification.Such models should suffice to predict the dynamic behavior of large biological systems, such as cancer molecular mechanisms.

Consequently, our work shifted focus to relative stability and dynamic sensitivity analysis.The power-law structure of S-systems simplifies the calculation of steady-state values and sensitivity (solved via algebraic equations [19, 20]. Voit and colleagues further explored operational criteria for transitioning from an original steady state to a new target state using linear algebra and linear programming [21]. We introduced root locus concepts to analyze the impact of system parameters on stability [22], directly conducting sensitivity analysis on dynamic behavior[23, 24]. We then establish stability criteria for S-systems to determine the environmental conditions under which these systems remain stable [25].Yet two fundamental challenges hinder S-system application: the pervasive sloppiness of kinetic parameters [26], and the lack of systematic methods to derive operating principles for biological control [27]. Parameter sloppiness manifests when vastly different kinetic constants yield nearly identical system behaviors—a property potentially advantageous for evolutionary robustness [28] but complicating parameter estimation and experimental design. Recent studies reveal that biological system models (e.g., mass action kinetics and Michaelis-Menten systems) are generally sloppy [26, 29] with parameter variations of several orders magnitude often having minimal impact on output. While some scholars argue against precise parameter estimation [30-32], others demonstrate that sloppiness doesn't preclude identifiability [33], and geometric analyses show sloppy models remain bounded even at parameter extremes [34].Concurrently, deriving operating principles governing biological state transitions remain largely ad hoc despite importance for synthetic biology and therapeutic interventions [10].

Visualization offers a powerful pathway to address these dual challenges. By transforming high-dimensional parameter spaces into intuitive representations, we can identify geometrically degenerate dimensions, isolate control-relevant parameters, and bridge abstract modeling with experimental implementation. Recent advances in topological data analysis [35] and interactive visual analytics [36] provide crucial tools for decoding these complex relationships when adapted to S-systems.This paper introduces a unified framework that combines computational approaches with visualization techniques to tackle S-system challenges. We demonstrate how (a)Hessian matrix construction in Simulink reveals hierarchical parameter sloppiness spectra, (b)control-theoretic methods extract biologically interpretable operating principles, (c)interactive visualization tools create biologist-friendly computational environments, and (d) graphical modularization facilitates cross-disciplinary collaboration.Our work establishes visualization not merely as an explanatory aid, but as a discovery engine that transforms S-system complexities into actionable design insights for synthetic biology and precision medicine applications. By breaking through current analytical bottlenecks, we enable researchers to navigate the intricate landscape of biological system sloppiness while deriving practical control strategies for therapeutic interventions.

II. METHODS

We now concentrate on three pivotal challenges in S-system biology. (*Quantifying sloppiness*) Through Hessian matrix construction in Simulink, we compute parameter sensitivity spectra to reveal hierarchical sloppiness in S-system dynamics (Fig. 8). (*Deriving operating principles*) We establish control-theoretic methods to extract biologically interpretable design rules from these nonlinear systems (Section III-2). (*Visualization*) Breaking through current bottlenecks in systems analysis by developing graphical modularization techniques to create user-friendly interfaces which facilitate cross-disciplinary collaboration for biologist-oriented computational environments.This integrated approach bridges theoretical systems biology with actionable insights for synthetic biology applications.

II-1 Sloppiness Analysis of S-Systems

Recent studies have revealed that dynamic biological system models (e.g., mass action kinetics and Michaelis-Menten kinetics systems) are generally sloppy [26, 29]. This means that even variations in certain parameters by several orders of magnitude (decades) do not significantly affect system output. Chis and colleagues examined the relationship between sloppiness and structural/practical identifiability through case studies, concluding that sloppiness does not imply a lack of identifiability and that sloppy models are indeed identifiable [37]. Transtrum and colleagues interpreted sloppy models from a geometric perspective, noting their bounded nature — even when parameters or parameter combinations approach extremes (0 or ∞), the results do not diverge to infinity [38]. Clearly, model sloppiness influences how systems should be handled and whether further model simplification via principal component analysis is necessary, underscoring its importance. Therefore, building on the sensitivity analysis from our previous paper [24], this study will investigate the sloppiness of S-systems to determine whether the kinetic parameters representing the net strength of component interactions are stiff.

Metrics for Measuring Model Sloppiness ($\boldsymbol{H}^{\aleph}$) :Brown introduced the Hessian matrix to explore the impact of parameter variations on the behavior of biological models with multiple parameters, defining sloppy and stiff parameters [29, 39] (sloppy parameters have minimal impact on system behavior even with large variations, while stiff parameters tightly constrain dynamic behavior). Gutenkunst and colleagues proposed the sloppy spectrum of parameter sensitivity to distinguish between sloppy and stiff models [26].Here, we use the function $\aleph(\theta)$ to quantify changes in model behavior due to parameter perturbations [26] (for *n* components and K experiments):

$$\aleph(\theta) = \frac{1}{2\mathrm{nK}} \sum_{k=1}^{k=K} \sum_{i=1}^{i=n} \frac{1}{T_k} \int_0^{T_k} \left[\frac{x_i^k(\theta,t) - x_i^k(\theta*,t)}{x_{i,max}} \right]^2 dt. \quad (2)$$

Although $\boldsymbol{H}^{\aleph}$ (Equation 3) is a local quadratic approximation of $\aleph(\theta)$, Brown′s extensive Monte Carlo-based principal component analysis of various models revealed that the sloppiness predicted by $\boldsymbol{H}^{\aleph}$ sufficiently represents the behavior of $\aleph(\theta)$. By substituting the S-system (Eq. 1),the elements of the corresponding Hessian matrix $H_{l,m}^{\aleph}$ can be derived as(where $\sigma_i = x_{i,max}$):

$$H_{l,m}^{\aleph} = \frac{\partial^2 \aleph(\theta)}{\partial log\theta_l \cdot \partial\, log\, \theta_m}|_{\theta^*}$$
$$= \frac{1}{\mathrm{nK}} \sum_{k=1}^{k=K} \frac{1}{T_k} \sum_{i=1}^{i=n} \frac{1}{\sigma_i^2} \int_0^{T_k} \left(\int_0^t \frac{\partial f_i^k(\theta^*,\tau)}{\partial log\theta_l} d\tau \right) \left(\int_0^t \frac{\partial f_i^k(\theta^*,\tau)}{\partial log\theta_m} d\tau \right) dt, \quad (3)$$

The power-law structure of S-systems further simplifies the differential terms:

$$\frac{\partial f_i^k(\theta^*,\tau)}{\partial log\alpha_i} = v_i^+,$$
$$\frac{\partial f_i^k(\theta^*,\tau)}{\partial log\beta_i} = -v_i^-,$$
$$\frac{\partial f_i^k(\theta^*,\tau)}{\partial log g_{ij}} = g_{ij} \cdot lnx_j \cdot v_i^+,$$
$$\frac{\partial f_i^k(\theta^*,\tau)}{\partial log h_{ij}} = -h_{ij} \cdot lnx_j \cdot v_i^+ \circ \quad (4)$$

Deriving Parameter Sloppiness Spectra via Hessian Matrix in Simulink: Using Equations (3) and (4), the $\boldsymbol{H}^{\aleph}$ for S-systems can be computed, and the parameter sloppiness spectrumcan be constructed from its eigenvalues. A model is considered sloppy if its eigenvalue distribution spans more than three orders of magnitude. To make this accessible to biologists, we will use block diagrams to compute the Hessian matrix and generate the sloppiness spectrum, with simulations conducted in the Simulink environment. FigureS1 of Supplementshows the *sloppiness spectrum* we previously established for dynamic behavior ***near steady states*** [15]. FigureS2 of Supplementdisplays the modular block diagram for *dynamic sensitivity* of S-systems developed in our previous paper [24], which will serve as the foundation for constructing the Hessian matrix and parameter sloppiness spectrum for S-system dynamic behavior.Tests will be conducted using small to medium-sized biological systems (n =3, 4, 5, 20, and 30 genes) to examine whether the dynamic behavior of S-systems at arbitrary points remains stiff, as observed near steady states.

II-2 Operating Principles for S-Systems Based on Control Theory

In recent years, design principles have become a popular research topic, yet their dynamical counterpart—operating principles—has received only modest attention [40]. Here, we employ control-theoretic techniques to address a critical scenario: when a biological system is subjected to external stress, necessitating a shift in its steady state from nominal conditions to target states, how should the independent variables be configured to achieve this requirement?

By defining augmented variables($y_j = \ln x_j$, $a_{ij} = g_{ij} - h_{ij}$, $b_i = \ln(\beta_i - \alpha_i)$) for the S-system in Eq. (1), its steady state can be expressed as $A_D Y_D + A_I Y_I = b$, where the system matrix for dependent variables $A_D = \begin{bmatrix} a_{11} & \cdots & a_{1n} \\ & \vdots & \\ a_{n1} & \cdots & a_{nn} \end{bmatrix}$, the system matrix for independent variables $A_I = \begin{bmatrix} a_{1,n+1} & \cdots & a_{1,n+m} \\ & \vdots & \\ a_{n,n+1} & \cdots & a_{n,n+m} \end{bmatrix}$, the dependent variable $Y_D = \begin{bmatrix} y_1 \\ \vdots \\ y_n \end{bmatrix}$, the independent variable $Y_I = \begin{bmatrix} y_{n+1} \\ \vdots \\ y_{n+m} \end{bmatrix}$, and the constant vector $b = \begin{bmatrix} b_1 \\ \vdots \\ b_n \end{bmatrix}$. The steady-state relationship becomes $A_I Y_I = b - A_D Y_D$, where Y_D is the target state and the parametric matrix A_I, A_D, b are known. Three solution scenarios[40]—unique ($n = m$), non-existent ($n > m$), or infinite ($n < m$)—are defined by the steady-state algebraic relation between dependent and independent variables. For the no-solution case ($n > m$), Voit and colleagues partitioned dependent variables into primary and secondary categories, correspondingly split the matrix L for $L \cdot Y_I = Y_D'$ (where $Y_D' = Y_D - {A_D}^{-1} b$ and $L = -{A_D}^{-1} \cdot A_I$),and prioritized driving the primary variables toward targets while sacrificing secondary variables. For the infinitely-many-solutions case ($n < m$), they employed matrix inversion or mixed-integer linear programming to identify admissible solutions [40]. Voit and colleagues addressed the non- and infinite-solution cases *statically* ($n > m$ and $n < m$): approximating solutions for unsolvable systems by prioritizing key variables and optimizing for underdetermined systems[40]. In contrast, *we shift the focus from static analysis to the underlying dynamic behavior. We investigate what forms of independent variables are dynamically feasible and naturally preferred by biological systems.*

Control Framework: System control fundamentally involves designing controllers to ensure system outputs align with desired values. The operating principle, in this context, is to identify the independent variables($x_j(t), j = n+1, \cdots n+m$)of the S-system such that the steady state of the dependent variables($x_j(t), j = 1, \cdots n$)ransitions from nominal values to specified target values. Thus, independent variables are treated as system inputs ($u(t)$), while dependent variables are regarded as system state variables. A controller is designed to drive the state variables from their initial (nominal) values to the desired steady state (target values). The controller output (system input) that sustains this new steady state corresponds to the independent variable values required for the new state.If the system is fully controllable, there always exists an input variable ($u(t)$) capable of steering the system from its initial state to the specified target. If the system is not fully controllable, we seek the best approximate solution.Grounded in this control framework, this study aims to develop an operator to establish operating principles for S-systems.

Linear Quadratic Regulator (LQR):We shall design a traditional linear quadratic regulator to provide a operating principle under linearized S-systems. The S-system model was linearized around nominal operating points using Jacobian linearization techniques to obtain state-space representations ($X(t) = A\dot{X}(t) + Bu(t)$). The cost function $J = \int (X^T(t) Q X(t) + u^T(t) R u(t)) dt$ was minimized, where Q and R represented state and control weighting matrices, respectively. The Riccati equation was solved to obtain the optimal feedback gain matrix K, yielding the control law $u(t) = -KX(t)$. The ***lqr***function of the Matlabis used to get the feedback gain: $K = \boldsymbol{lqr}(A, B, Q, R)$.

Optimal Fuzzy Control for Nonlinear Systems: Linear quadratic regulator control provides theoretically optimal performance for linear systems, while fuzzy control offers superior robustness and nonlinear approximation capabilities. By integrating these approaches, the previously proposed optimal fuzzy controller—built upon Takagi-Sugeno(T-S) fuzzy systems—combines their respective strengths [41, 42]. This method is particularly advantageous for nonlinear physical and biological systems represented by T-S fuzzy models.The T-S fuzzy model is formulated as follows (whereR^idenotes the ith rule of the fuzzy model,$i = 1, \ldots r$.):

$$R^i: \text{If} x_1 \text{is} T_{1i}, \ldots, x_n \text{is} T_{ni}, \text{ then} \dot{X}(t) = A_i(t)X(t) + B_i(t)u(t), \; Y(t) = C(t)X(t), \quad (5)$$

where $x_1 \ldots, x_n$are system states, $T_{1i}, \ldots T_{ni}$are fuzzy terms, and $u(t)$ and $Y(t) = [y_1, \ldots y_{n'}]^T$ denote system input vectors and output vectors, respectively.The corresponding fuzzy controller is designed in the form:

$$R^i: \text{If} y_1 \text{is} S_{1i}, \dots, y_{n'} \text{is} S_{n'i}, \text{ then } u(t) = r_i(t), \ i = 1, \dots \delta, (6)$$

where $S_{1i}, \dots S_{ni}$ are fuzzy sets for the controller inputs. The locally asymptotically optimal control law is given by [41, 42]:

$$r_i^*(t) = -B_i^T \bar{\pi}_i X^*(t), (7)$$

and the globally optimized control signal $u^*(t) = \sum_{i=1}^{r} h_i \left(X^*(t)\right) r_i^*(t)$ is obtained through fuzzy blending, which minimizes the quadratic cost function $J\left(u(\cdot)\right) = \int_0^\infty (X^T(t) Q X(t) + u^T(t) R u(t)) dt$.

Here, $X^T(t)QX(t)$ penalizes state deviations, $u^T(t)Ru(t)$ regulates control effort,and Q, R are symmetric positive semidefinite weighting matrices. This formulation transforms the optimization problem into a recursive dynamic programming structure [42].The fuzzy subsystems (5) and control rules (6) exhibit a one-to-one correspondence (i.e., the *i*-th rule pair), and the overall system behavior emerges from the fuzzy blending of all subsystems. This optimal fuzzy control framework has been successfully applied to diverse systems, including magnetic suspension systems, 4-pole and 8-pole active magnetic bearings, inverted pendulums, half-car active suspensions, and the Taiwan iTS-1 experimental vehicle.

II-2 Simulink-Based Visualization for Biological Systems Analysis

Simulink (MathWorks®) is a computational modeling environment within the MATLAB (MATrixLABoratory) framework that implements a block diagram paradigm for dynamic system analysis and design [23-25]. This toolbox provides an interactive platform to construct block diagrams representing multi-domain dynamic systems, where biological components are abstracted as functional blocks and dynamic interactions (e.g., metabolic fluxes, regulatory signals) are encoded via directed signal lines. The graphical interface eliminates low-level programming requirements while maintaining mathematical rigor through automated backend computations, enabling researchers to achieve modeling, simulation, and analysis of complex biological networks.Key features of Simulink for biological applications include dynamic sensitivity analysis (native tools for parametric sensitivity computation, including automated Jacobian calculation for sensitivity matrices, enabling quantification of parameter influence on system behavior), multi-domain simulation (unified modeling of heterogeneous processes, including biochemical reaction networks, control-theoretic constructs, and stochastic processes, through modular block libraries), visual analytics (real-time visualization of state variable trajectories, parameter perturbation effects, and sensitivity metrics, facilitating intuitive exploration of system dynamics), and adaptive numerical solvers (robust solvers tailored for stiff biological systems such as ODEs with widely varying time scales, ensuring numerical stability and accuracy).The environment supports exportable block libraries for modular network design, allowing researchers to build reusable, scalable models while maintaining direct access to underlying mathematical operations (e.g., Hessian matrix computation for sloppiness analysis). This combination of visual accessibility and computational power makes Simulink particularly suited for interdisciplinary teams seeking to bridge theoretical models with experimental validation in systems biology.

III. RESULTS AND DISCUSSION

This section presents a comprehensive evaluation of the proposed computational framework for analyzing sloppiness and deriving operating principles in S-system models of biological networks. The results are structured into three main parts: First, we quantify the inherent parameter sloppiness across S-systems of varying complexity (3 to 30 genes) using Hessian-based sensitivity spectra simulated in Simulink. Second, we demonstrate the efficacy of LQR-based control strategy in steering system dynamics from nominal to target steady states, effectively establishing practical operating principles for biological intervention. The performance of the proposed operating principles will be validated using the three-tier cascade pathwaysystem ($n = 3 > m = 1$, no-solution case) and a branched pathway with a substrate cycle system ($n = 4 < m = 7$, infinite-solution).Finally, we showcase our optimal fuzzy control approach, which integrates the robustness of fuzzy logic with the precision of optimal control theory for operating principle.

III-1 Sloppiness Analysis of S-Systems

We investigated the sloppiness of S-systems using five biological genetic networks of varying size of dependent variable ($n = 3, 4, 5, 20, 30$ in Fig. 1). The related S-system representation is shown in the right column of Figure S3 in Supplement. To address the computational challenges associated with solving the highly complex integrals required for Hessian matrix calculations in these highly nonlinear systems, we implemented a control-theoretic block diagram approach in Simulink.We first demonstrate this visualization-driven sloppiness analysis using a three-tier cascade pathway (upper-left panel in Fig. 1 [43-47]). Building on our prior

work in *dynamic sensitivity analysis* (Figure S2 in Supplement [24]), we integrated Equations (1), (3) and (4) to compute the Hessian matrix $\boldsymbol{H}^{\aleph}$ for the S-system. To enhance accessibility for biologists, we designed a user-friendly block diagram in Simulink (lower panel of Figure 3) to numerically construct the Hessian matrix. Figure 2 shows the generated parameter sloppiness spectra. Figure 3 is the workflow efficiently derives the corresponding eigenvalues, enabling the generation of parameter sloppiness spectra.

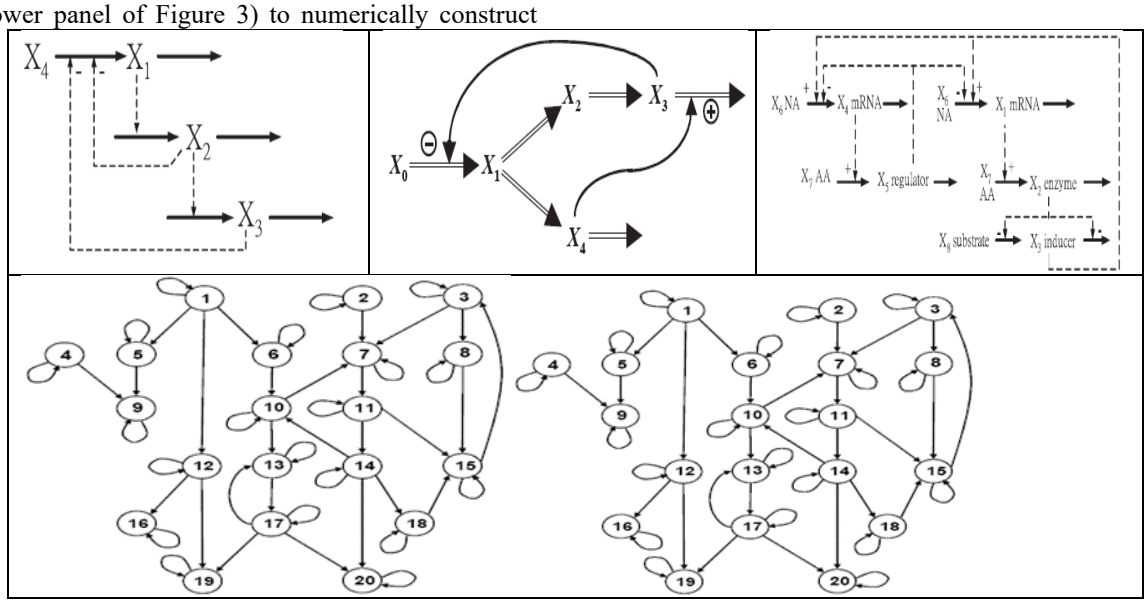

Figure 1: Biological systems for validating S-system sloppiness [43-47]

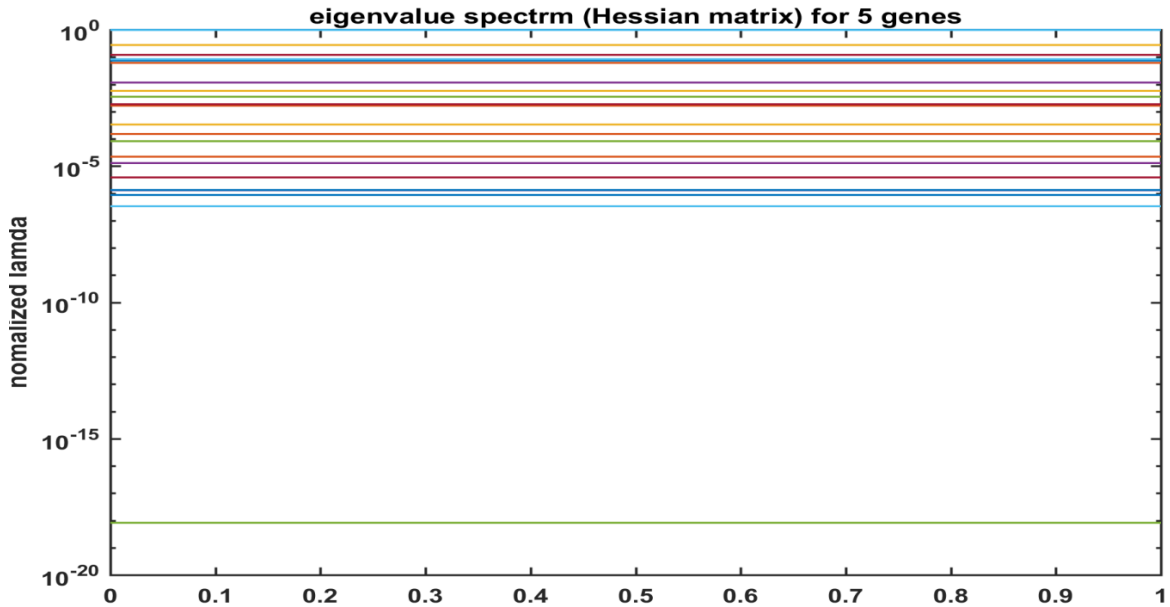

Figure 2: Parameter sloppiness spectrum of thethree-tier cascade pathway.

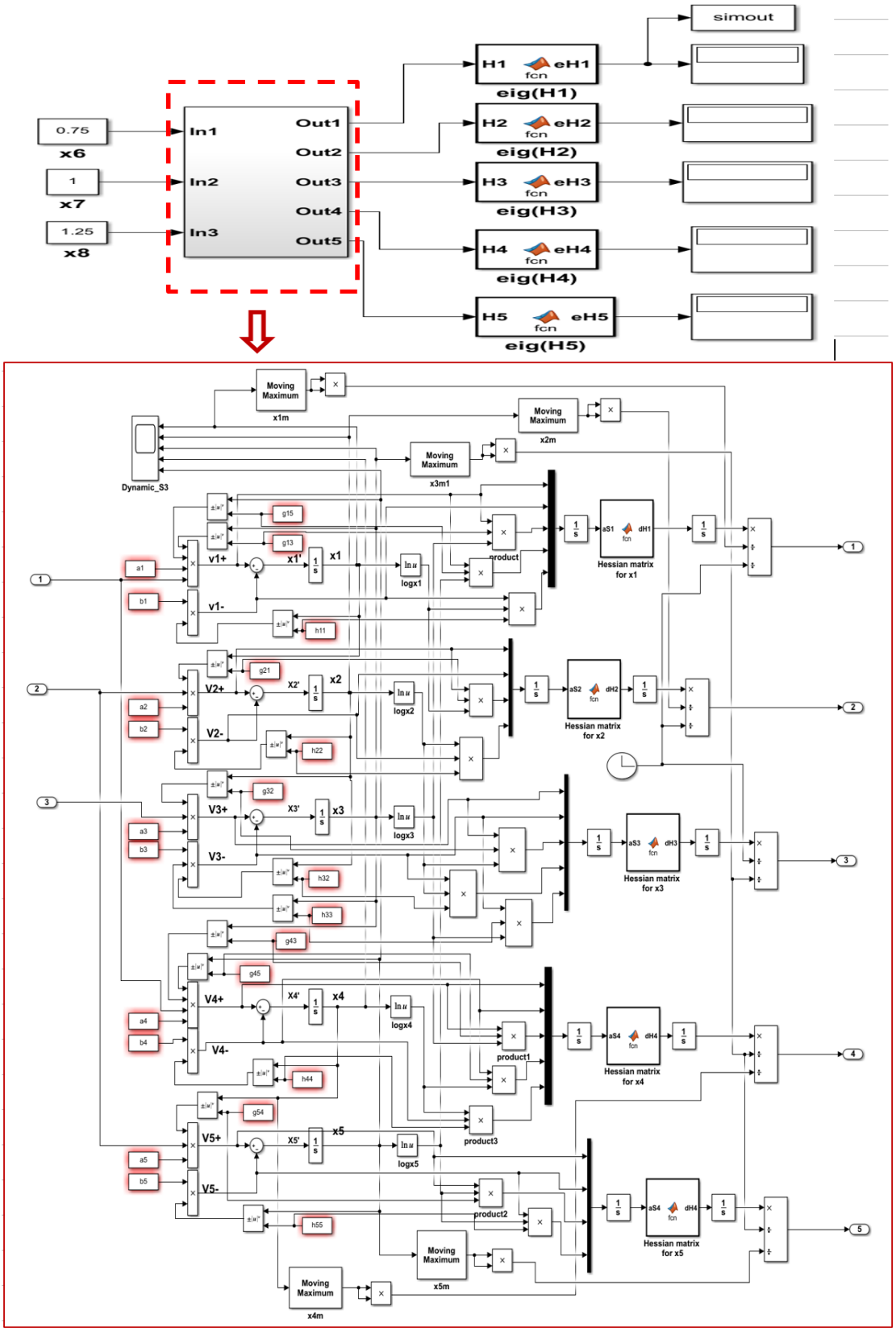

Figure 3: Block diagram for sloppiness analysis of the three-tier cascade pathway.

Furthermore, the proposed visualization technique was extended to large-scale systems. Figure 4 illustrates the dynamic behavior of the 30-gene network, based on which the corresponding sloppiness (Equations (3) and (4)) were derived. Figure 5 displays the simulated parameter sloppiness spectrum for the 30-gene system: 76 out of 128 curves fall within [10^{0}, 10^{-3}], while 127 out of 128 curves lie within [10^{0}, 10^{-6}]. Figure 6 shows the block diagram for sloppiness analysis of the 30-gene network system.For this large-scale system, subsystems were employed to simplify the block diagram. Figure 7 is the workflow for the corresponding eigenvalues enabling the generation of parameter sloppiness spectra, where the blocks HeXi (i = 1, ..., 30) correspond to the output results shown in Figure 6. Figure 8 shows the parameter sloppiness spectra for the five S-system biological systems depicted in Figure 1. *The results indicate that while dynamic behavior at arbitrary points exhibits a less concentrated sloppiness spectrum compared to that near steady states, stiffness is still present. This implies that perturbation in each kinetic parameter will influence the system's dynamic behavior.*

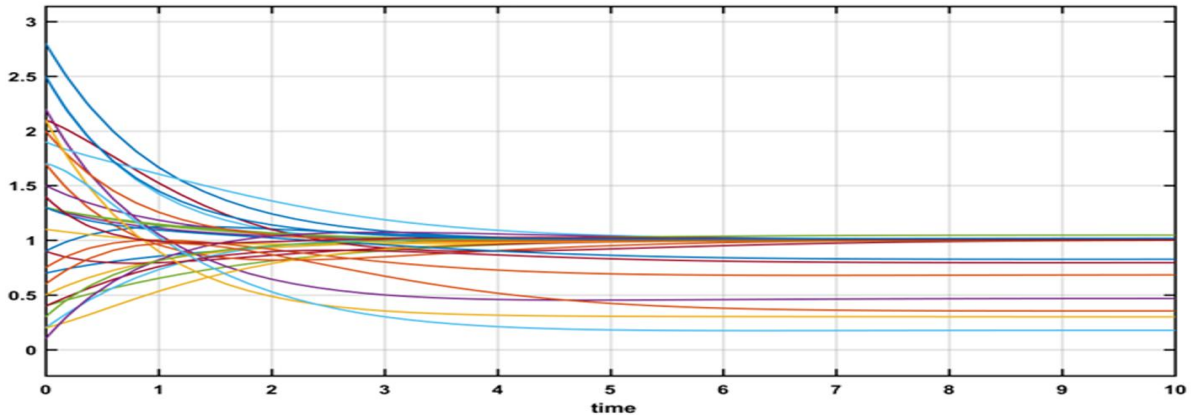

Figure 4: Dynamic behavior of the 30-gene network system.

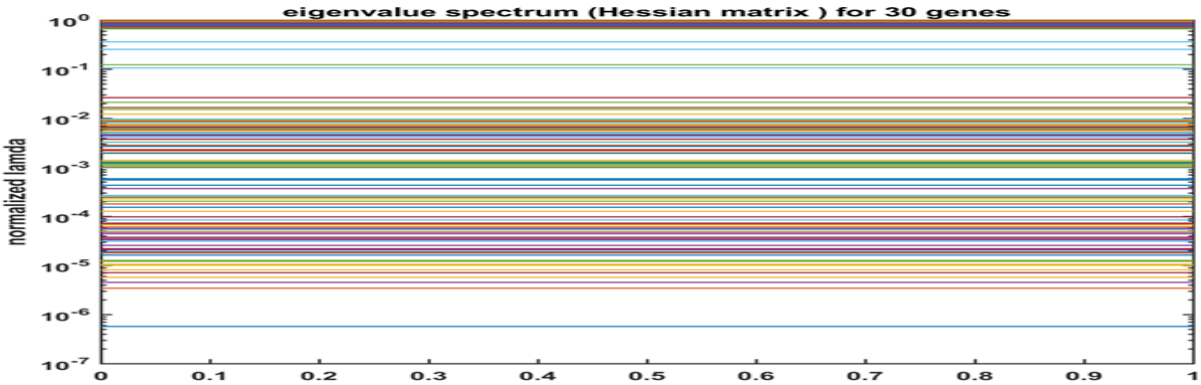

Figure 5: Parameter sloppiness spectrum of the 30-gene network system.

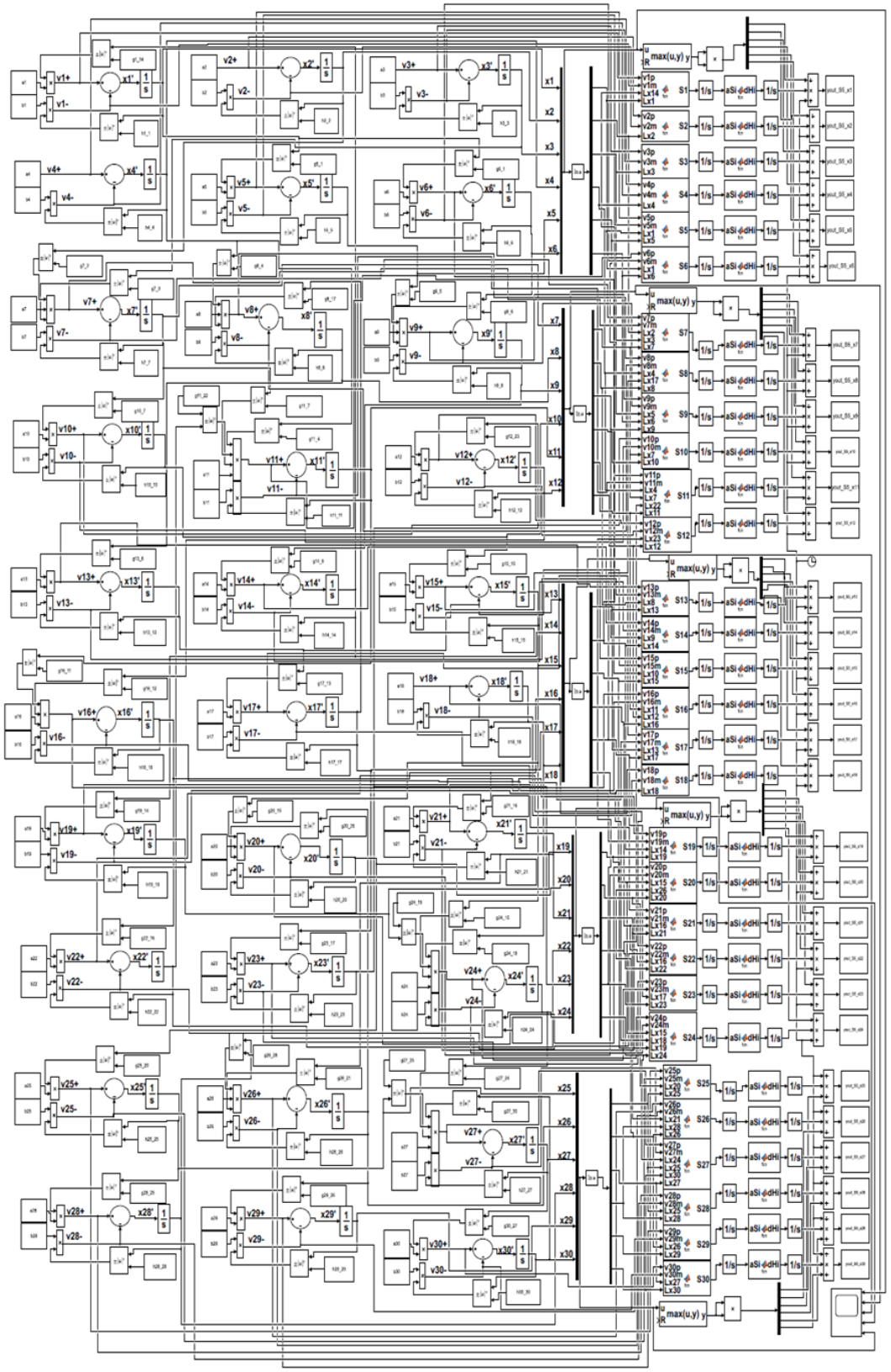

Figure 6: Block diagram for sloppiness analysis of the 30-gene network system.

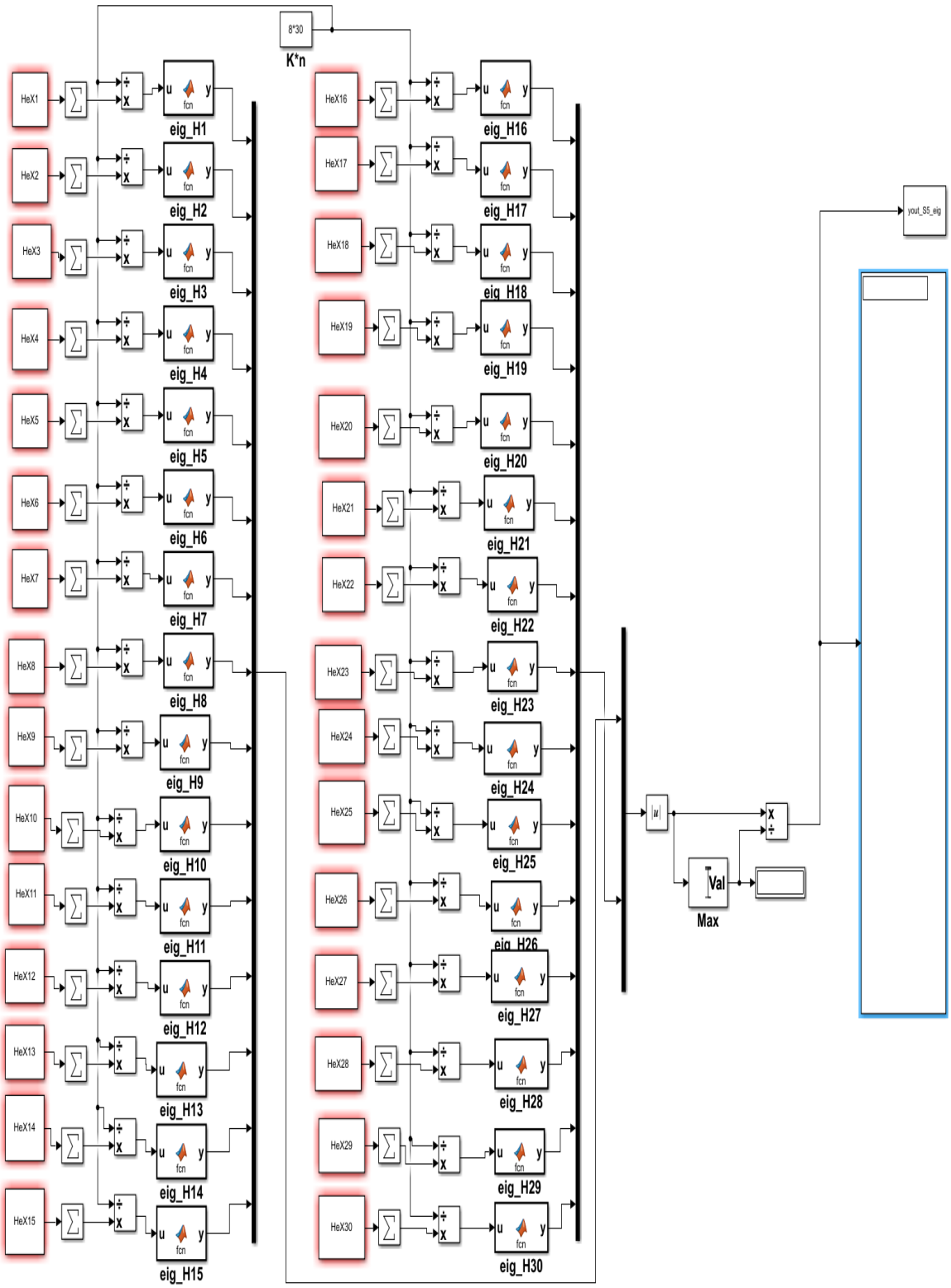

Figure 7: Block diagram to estimate eigenvalues of Hessian matrixfrom Fig. 6,denoting sloppiness analysis of the 30-gene network system.

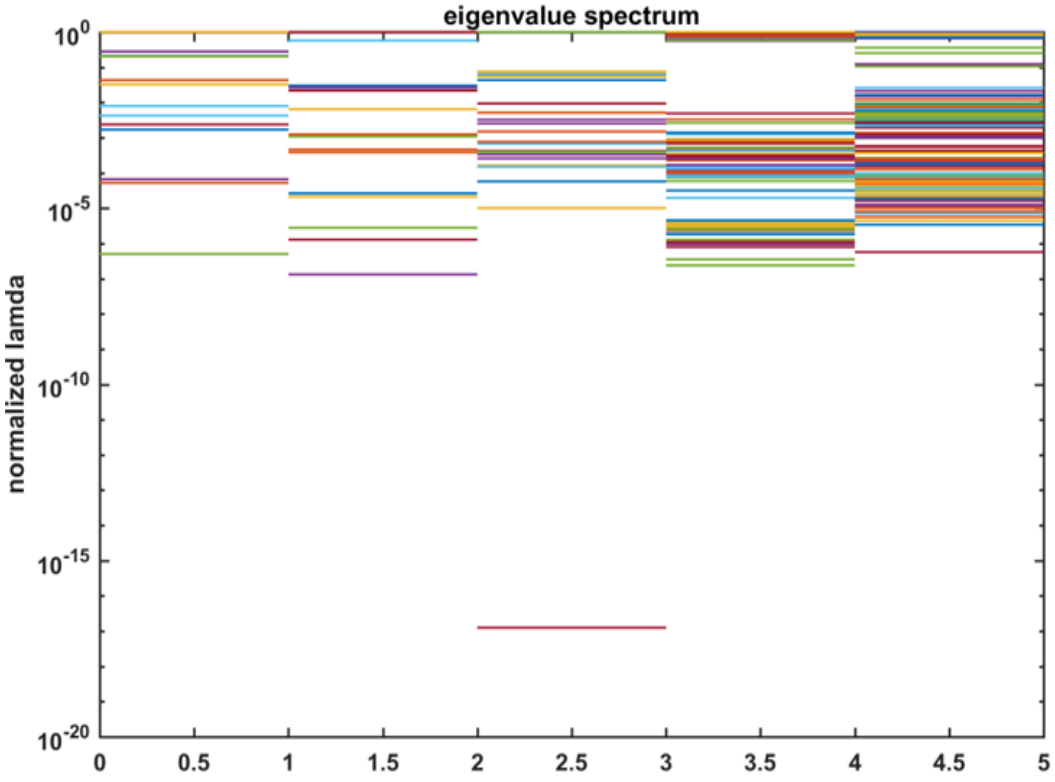

Figure 8: Parameter sloppiness spectra of small to medium-sized S-system biological systems in Fig. 1.

III-2 Operational principle of S-Systems

Here, we employ two control techniques—linear quadratic regulator (LQR) and optimal fuzzy control—to establish operating principles for S-system biological models. System control involves designing controllers to ensure system outputs match desired values, while operating principles focus on identifying independent variables that shift the steady state of dependent variables from nominal values to specified targets. Thus, independent variables are treated as system inputs, and dependent variables as system states. The controller is designed to drive state variables from their initial (nominal) values to the target steady state. The controller output (system input) that maintains this new steady state corresponds to the independent variable values required for the new state.If the system is fully controllable, there always exists an input that drives the system from its initial state to the specified target. If the system is not fully controllable, we seek the best approximate solution. To validate the performance of the proposed control-based operating principles, we consider two systems: athree-tier cascade pathway in the upper-left panel of Fig.1($n = 3$ and $m = 1$, no solution exists) and a branched pathway system with a substrate cyclein Fig. 9($n = 4$ and $m = 7$, infinitelymany solutions exist).The case $n = m$ (unique solution) is omitted here as it is straightforward.

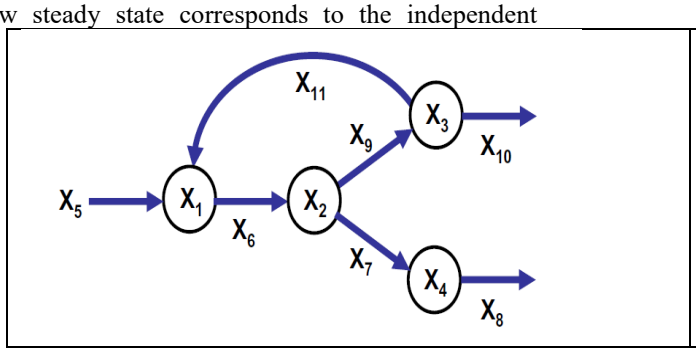

$$\dot{x}_1 = \alpha_1 x_3^{g_{13}} x_5^{g_{15}} x_{11}^{g_{1,11}} - \beta_1 x_1^{h_{11}} x_6^{h_{16}},$$
$$\dot{x}_2 = \alpha_2 x_1^{g_{21}} x_6^{g_{26}} - \beta_2 x_2^{h_{22}} x_7^{h_{27}} x_9^{h_{29}},$$
$$\dot{x}_3 = \alpha_3 x_2^{g_{32}} x_9^{g_{39}} - \beta_3 x_3^{h_{33}} x_{10}^{h_{3,10}} x_{11}^{h_{3,11}},$$
$$\dot{x}_4 = \alpha_4 x_2^{g_{42}} x_7^{g_{47}} - \beta_4 x_4^{h_{44}} x_8^{h_{48}}. \quad (8)$$

Figure 9:Branched metabolic pathway with a substrate cycle, adapted from [40].

LQR-based operating principle:When identifying the operating principles for S-systems, the independent variables serve as inputs to the computing system and simultaneously as system inputs. In practice, this configuration is*inherently unworkable*. However, since the goal of deriving operating principles is solely to find a solution rather than to achieve real-time operation, the inputs to the biological system can be delayed before being fed into the computing system (Figure 10).We first examine the three-tier cascade pathway in the upper-left panel in Fig. 1. **Table 1** compares simulation results with target values for the serial system (independent variable $x_4 = u(t), \boldsymbol{n = 3} > m = 1$). The results show a strong agreement between the desired and estimated states, confirming the method's efficacy even for inherently unsolvable cases. Figure 10 shows the block diagram for implementing operating principles in the three-tier cascade pathwaysystem, with independent variable values highlighted in red circles. We further use the branched pathway system with a substrate cycle in Fig. 9 to examine the infinite-solution case ($\boldsymbol{n = 4} < m = 7$). Figure 11 presents the block diagram for the branched pathway system, and Figure 12 displays the dynamic behavior of the system state variables x_1, x_2, x_3, x_4 .The controller achieves a close fit between the target and simulated outputs (highlighted in red circles), effectively resolving the infinite-solution condition. These demonstrates that for systems where no exact algebraic solution exists ($n > m$ and $n < m$), the proposed control strategy successfully achieves a close approximation between the desired and estimated steady states.

desired states	**estimated states**	Control output, u(t) (**estimated x_4**)
[5.3294,10.2805,1.7848]	[5.31 10.24 1.778]	1.496
[15.4812,29.8633,5.1846]	[15.49,29.69,5.152]	2.996
[57.0061,109.9655,19.0912]	[56.95, 109.7, 19.04]	6.993

Table 1:(**LQR**) Results of operating principles for the three-tier cascade pathway

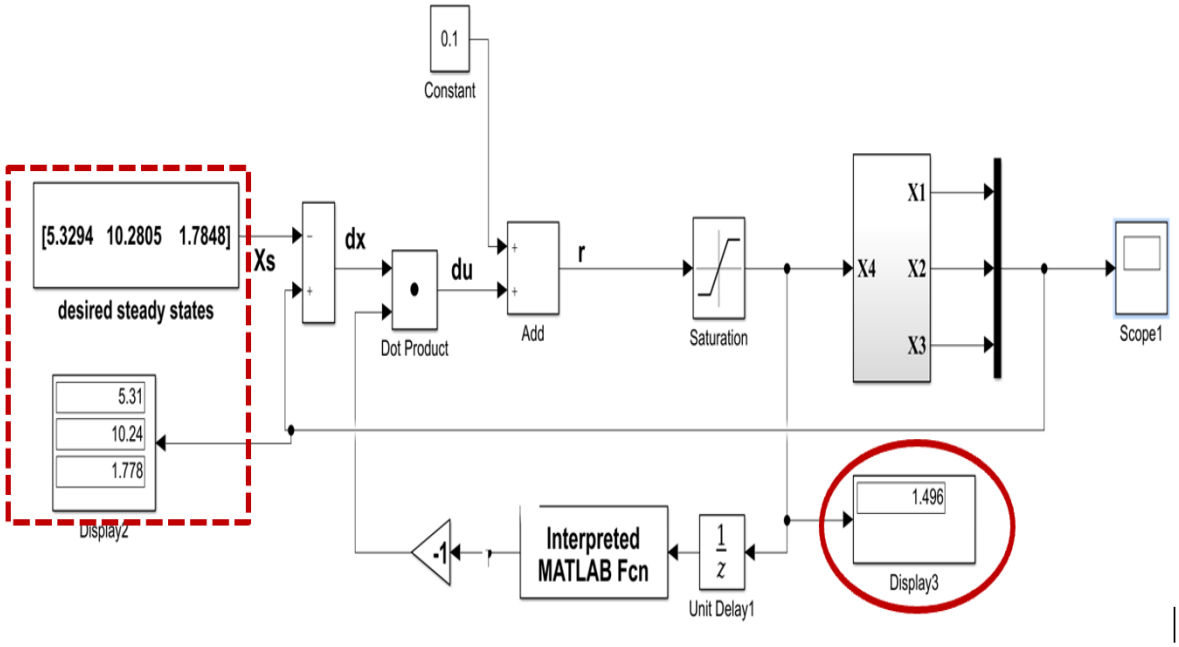

Figure 10: (**LQR**) Block diagram for operating principles of the three-tier cascade pathway.

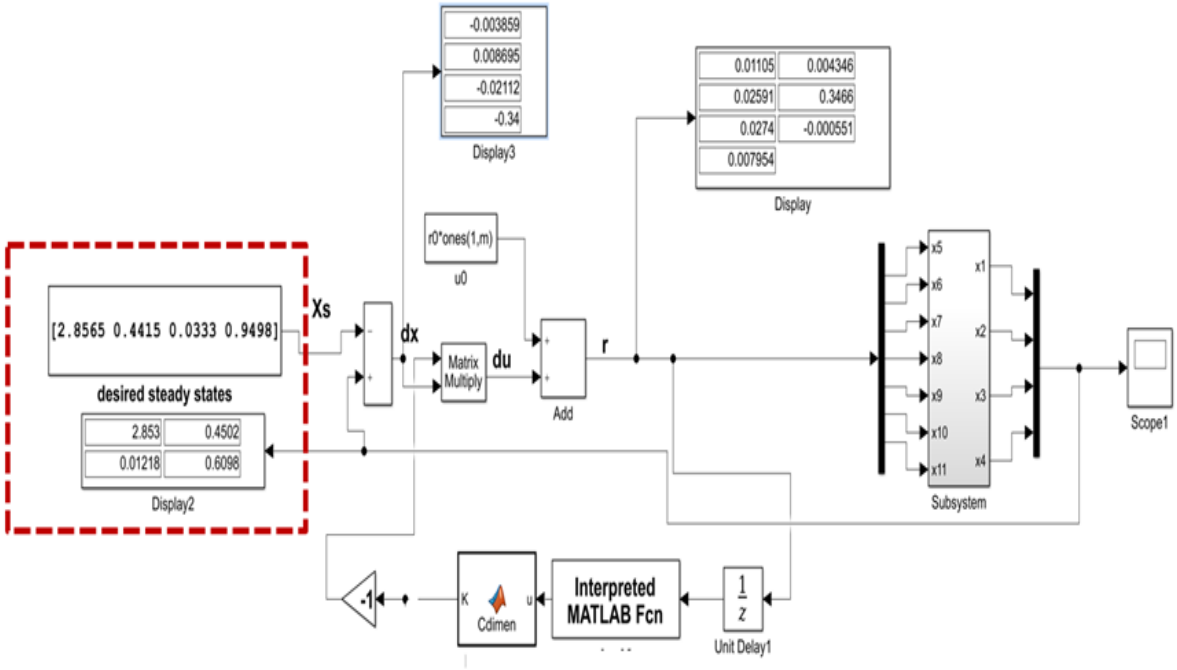

Figure 11:(**LQR**) Block diagram for operating principles of branched pathwayin Fig. 9.

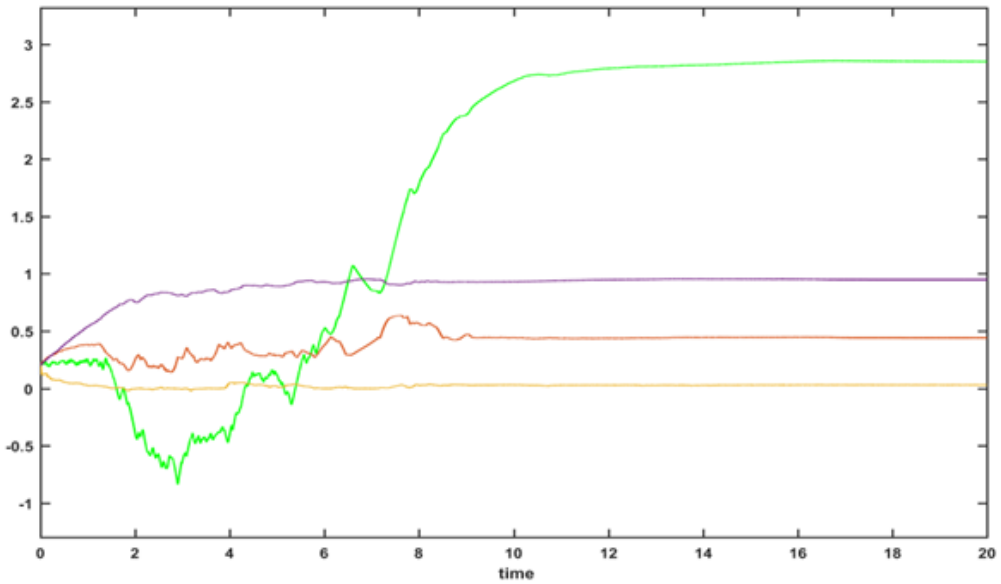

Figure 12:(**LQR**) System states$x_1, x_2, x_3, x_4$for the branched pathway in Fig. 9.

Optimal fuzzy control-based operating principle: The concept of sector nonlinearity transformation is intuitively simple but becomes computationally cumbersome for multivariate systems. Given that biological systems typically involve numerous variables, the method proposed by Kanaka and Wang [48] is unsuitable for such applications. In our 2013 work on modeling cancer molecular mechanisms [49], we developed a fuzzy system framework accounting for tissue environmental variations in multi-branch growth signaling pathways. Here, a Takagi-Sugeno (T-S) fuzzy system can be interpreted as a nonlinear system formed by blending multiple linear subsystems—each representing local characteristics (regions)—through fuzzy inference. Each local characteristic corresponds to a specific tissue environment or experimental condition as conceptualized in [49].For S-systems, Equation (9) or fuzzy rule (10) describes dynamic behavior near a steady state under a specific experimental condition:

$$\dot{z}(t) = \left(A_{D\circ}\ \ E\right)z(t) + \left(A_{I\circ}\ \ F\right)u(t) = \mathring{A}z(t) + \mathcal{B}u(t). \quad (9)$$

RuleR^l: IFu_1 is A_l, u_2 is B_l, …, u_m is M_l,then

$$\dot{z}(t) = \mathring{A}_l z(t) + \mathcal{B}_l u(t). (10)$$

In contrast to typical fuzzy modeling approaches—such as linearizing inverted pendulum systems at extreme angles (0° and 180°) [50] or cruise control systems at speed extremes (V^{max} and V^{min}) [51]—where nonlinear systems become linear at boundary values, S-systems remain nonlinear even under extreme experimental conditions. The locally linearized Equation (9) only approximates dynamics near steady states under specific conditions. Thus, fuzzy blending in this context can only represent behavior near steady states across various experimental conditions, not global nonlinear dynamics.In 2000, we derived an energy-based framework demonstrating a one-to-one correspondence (***i*-to-*i***) between optimal fuzzy controllers (Equations 6 and 7) and T-S fuzzy systems (Equation 10), leading to simplified control laws [41, 42]. However, these mathematical formulations remain inaccessible to many biologists. To address this, we have developed a modular graphical representation (Figure 13) to improve interpretability. The independent variable, x_4, and the deviation from a nominal states, E_xs1, are used as inputs of fuzzy controllers.A practical challenge arises because independent variables serve as both inputs to the fuzzy inference system and system inputs, creating implementation conflicts. To resolve this, we delayed system inputs before feeding them into the fuzzy inference system. While predictive compensation was initially attempted, its performance was unsatisfactory. Instead, we incorporated real-time error feedback to mitigate delay effects and generate immediate corrective control actions.Since the problem of *infinite solutions* ($n < m$) only requires finding *one set of independent variables* that drives the system variables to the target values, we focus here on validating the method for the **non-solution case (n > m)**.Table 2 shows a simulation comparing results with target values for the three-tier cascade pathwayin the upper-left panel of Fig.1(independent variable $x_4 = u(t), \boldsymbol{n} > m$). Figure 13 displays the block diagram and the identified x_4 values with a comparison between the estimated states and desired states(highlighted in red circles).The controller achieves a close fit between the target and simulated outputs, effectively resolving the non-solution condition.

desired states	**estimated states**	Control output, u(t) (**estimated x_4**)
[8.2965 16.00402.7785]	[8.2710 15.94272.7676]	2
[15.481229.86335.1846]	[15.4926 29.69155.1513]	3

Table 2: (**Fuzzy controller**) Simulation results vs. target valuesfor the three-tier cascade pathway.

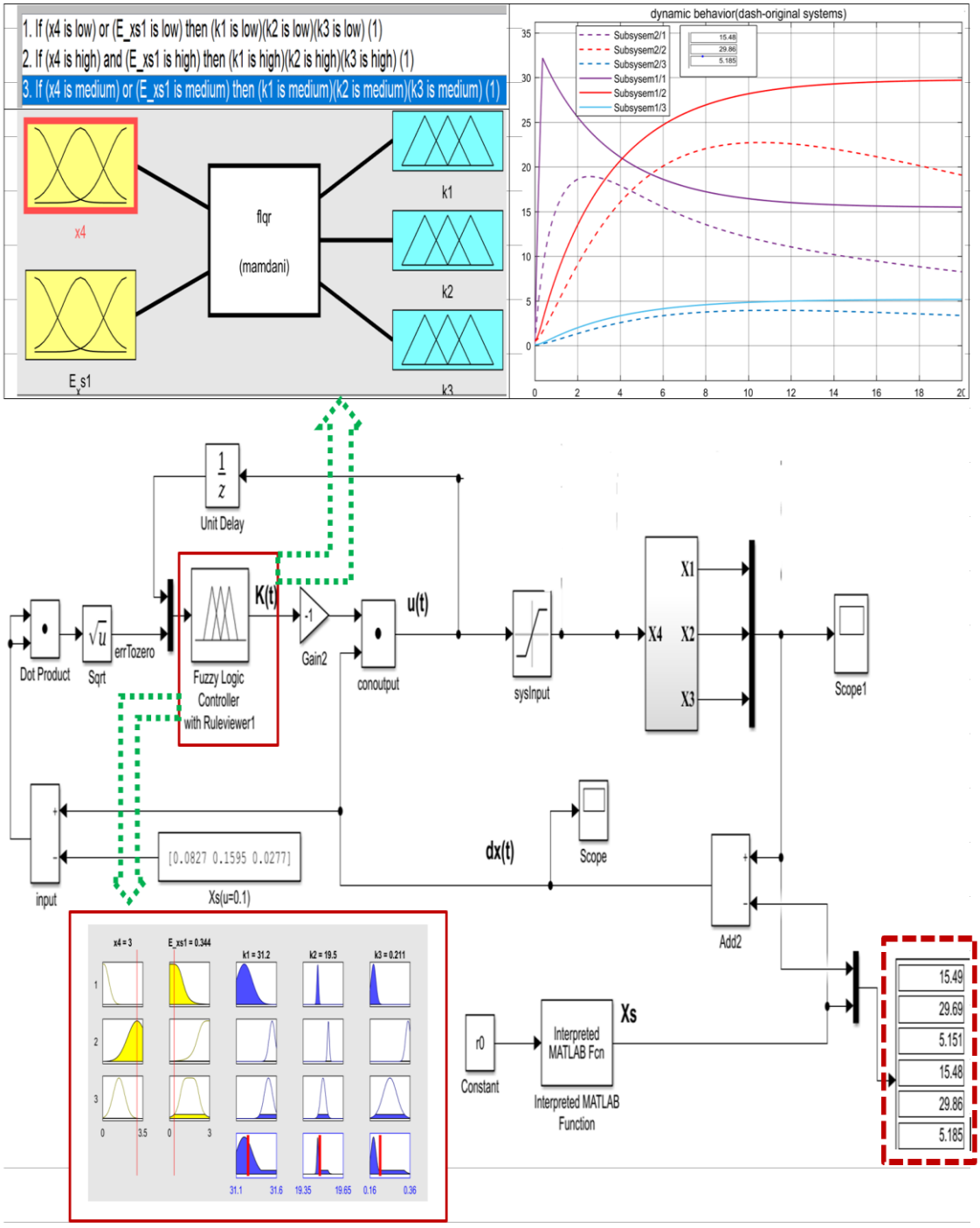

Figure 13:(Fuzzy controller) Block diagram for operating principles of the three-tier cascade pathway.

IV. CONCLUSION

This study successfully addressed the dual challenges of parameter sloppiness and operating principle derivation in S-system models of biological networks. By integrating control-theoretic frameworks with advanced visualization techniques, we developed a unified computational approach to transform these theoretical obstacles into actionable biological insights.Our key contributions are threefold.(*Visualization of sloppiness*) We implemented a Simulink-based Hessian matrix workflow to quantify and visualize parameter sloppiness spectra across S-systems of varying complexity (3 to 30 genes). This approach revealed

that while large-scale systems exhibit extensive parameter sloppiness (e.g., 127 of 128 eigenvalues spanning six orders of magnitude in a 30-gene network), their dynamic behavior remains stiff—meaning perturbations in kinetic parameters consistently influence system output. This confirms that sloppiness does not preclude identifiability or controllability but necessitates geometric analysis of parameter manifolds. (*Control-theoretic operating principles*) We established that operating principles for biological intervention can be derived by reframing the steady-state transition problem as a control task. By treating independent variables as system inputs and dependent variables as states, we demonstrated that both LQR and optimal fuzzy controllers can effectively drive systems from nominal to target states—even for algebraically intractable cases ($n > m$ with no solution or $n < m$ with infinite solutions). The proposed fuzzy control architecture notably handled nonlinearities and multi-variable interactions more robustly than classical LQR. (*Biological interpretability*) Through modular block diagrams and interactive visual analytics, we bridged the gap between theoretical models and biological applicability. The graphical representation of sloppiness spectra and control laws provides biologists with an intuitive toolkit to explore parameter sensitivities, identify dominant regulatory interactions, and design targeted interventions—for instance, steering gene expression profiles in disease models.Future work will focus on developing real-time predictive compensation mechanisms to enhance the feasibility of *in silico* control strategies for experimental validation. Ultimately, this research underscores the power of interdisciplinary integration—leveraging control theory, computational visualization, and systems biology—to derive actionable principles for manipulating complex biological systems.

V. ACKNOWLEDGMENT

This research was supported by grant number MOST 109-2221-E-212-003 from the Ministry of Science and Technology of Taiwan, R.O.C.

REFERNCES

[1]. Bartocci E, Lió P (2016) Computational modeling, formal analysis, and tools for systems biology. PLoS Comput. Biol. 12(1):e1004591.
[2]. VoitEO (2013)Biochemical systems theory: A review. ISRN Biomathematics 2013:897658.
[3]. Sriyudthsak M, et al. (2016) Systems biology for analyzing metabolic processes in plants: A review. Front. Plant Sci. 7:1331.
[4]. Savageau MA (1976) Biochemical systems analysis: A study of function and design in molecular biology. Addison-Wesley.
[5]. Voit EO (2000) Computational analysis of biochemical systems: A practical guide for biochemists and molecular biologists. Cambridge University Press.
[6]. Tyson JJ (1991) Modeling the cell division cycle: cdc2 and cyclin interactions. Proc. Natl. Acad. Sci. USA 88:7328-7332.
[7]. Tyson JJ, Chen KC,NovakB (2003) Sniffers, buzzers, toggles and blinkers: dynamics of regulatory and signaling pathways in the cell. Curr. Opin. Cell Biol. 15:221-231.
[8]. Tavassoly I, ParmarJ, Shajahan-HaqA, Clarke R, Baumann W, Tyson JJ (2015) Dynamic modeling of the interaction between autophagy and apoptosis in mammalian cells. CPT Pharmacometrics Syst Pharmacol 4(4):263-72.
[9]. Liu S, Tao C, Huang Z, Huang S (2010) Modeling of p53 signaling pathway based on S-system equations. Journal of Biomedical Engineering 27(3):505-10 (Chinese)
[10]. Lim WA, et al. (2013) Design principles of regulatory networks: Searching for the molecular algorithms of the cell. Molecular Cell 49(2):202-212.
[11]. Kimura S, et al. (2005) Inference of S-system models of genetic networks using a cooperative coevolutionary algorithm. Bioinformatics 21(7):1154-1163.
[12]. Liu PK, Wang FS(2008) Inference of biochemical network models in S-system using multiobjective optimization approach. Bioinformatics 24:1085–1092.
[13]. Sarode KD, Kumar VR, Kulkarni BD(2016) Inverse problem studies of biochemical systems with structure identification of S-systems by embedding training functions in a gen etic algorithm. Mathematical Biosciences 275:93–106.
[14]. Wu SJ, Wu CT, Chang JY (2012) Fuzzy-based self-interactive multi-objective evolution optimization for reverse engineering of biological networks. IEEE Trans. Fuzzy Syst. 20(5):865-882.
[15]. Wu SJ, Wu CT (2013) Computational optimization for S-type biological systems: Cockroach genetic algorithm. Math Biosci. 245(2):299-313.
[16]. Wu SJ, Wu CT (2014) Seeding-inspired chemotaxis genetic algorithm for the inference of biological systems. Comput Biol Chem 53(2):292-307.

[17]. Wu SJ, Wu CT (2018) Smarten up computational intelligence to decipher time series data. Appl Soft Comput 72:442-456.
[18]. Wu SJ, Wu CT (2015) A bio-inspired optimization for inferring interactive networks: cockroach swarm evolution. Expert Syst Appl 42(6):3253-3267.
[19]. Wu CT, Wu SJ, Chang JY (2013) Computational analysis of S-type biological systems. Int. J. Eng. Res. Appl. 3(1):1976-1987.
[20]. Shiraishi F, Yoshida E, Voit EO (2014) An efficient and very accurate method for calculating steady-state sensitivities in metabolic reaction systems. IEEE/ACM Trans. Comp. Bio. Bioinfo. 11(6):1077-1086.
[21]. Lee Y, Chen PW, Voit EO (2011) Analysis of operating principles with S-system models. Math. Biosc. 231:49-60.
[22]. Wu SJ (2021) Root locus-based stability analysis for biological systems. J Bioinform Comput Biol 19(5): 2150023. https://doi.org/10.1142/S0219720021500232
[23]. Wu CT, Wu SJ, Chang JY (2022) Visualize dynamic sensitivity of biological systems. Int. J. Eng. Res. Appl.12(10):158-182.
[24]. Wu SJ, Lu SY (2025) Block-diagram implementation of S-system sensitivity analysis: A Simulink framework for power-law biological networks.Int. J. Eng. Res. Appl. 15(8):67-88.
[25]. Wu SJ, Wu CT (2018) Simulink-based analysis for coupled metabolic systems. Appl. Comput. Intell. Soft Comput. 2018:8075051.
[26]. Gutenkunst RN, et al. (2007) Universally sloppy parameter sensitivities in systems biology models. PLoS Comput. Biol. 3(10):e189.
[27]. Transtrum MK, Qiu P (2014) Model reduction by manifold boundaries. Phys. Rev. Lett. 113(9):098701.
[28]. Daniels BC, et al. (2008) Sloppiness, robustness, and evolvability in systems biology. Curr. Opin. Biotechnol. 19(4):389-395.
[29]. Brown KS, Sethna JP (2003) Statistical mechanical approaches to models with many poorly known parameters. Phys. Rev. E 68(2):021904.
[30]. Waterfall JJ, et al. (2006) Sloppy-model universality class and the Vandermonde matrix. Phys. Rev. Lett. 97(15):150601.
[31]. Mannakee BK, Ragsdale AP, Transtrum BK, Gutenkunst RN (2016) Sloppiness and the geometry of parameter space. in: Uncertainty in Biology, Springer, 271–299.
[32]. Kotte O, Heinemann1 M (2009) A divide-and-conquer approach to analyze underdetermined biochemical models. Bioinformatics 25(4):519–525.
[33]. Rand D (2008) Mapping global sensitivity of cellular network dynamics: sensitivity heat maps and a global summation law. J. R. Soc. Interf. 5:59–69.
[34]. Cirit M, Haugh JM (2012) Data-driven modelling of receptor tyrosine kinase signalling networks quantifies receptor-specific potencies of pi3k-and ras-dependent erk activation. Biochem. J. 441 (1):77–85.
[35]. CarlssonG (2009) Topology and data. Bull. Am. Math. Soc.46(2):255–308. https://doi.org/10.1090/S0273-0979-09-01249-X
[36]. Keim DA, Mansmann F, Schneidewind J, Ziegler H (2006) Challenges in visual data analysis. In Tenth International Conference on Information Visualisation (IV'06) (pp. 9-16). IEEE. https://doi.org/10.1109/IV.2006.31
[37]. Chis OT, Villaverde AF, Banga JR, Balsa-Canto E (2016) On the relationship between sloppiness and identifiability. Math. Biosci. 262:147-161.
[38]. Transtrum MK, et al. (2015) Perspective: Sloppiness and emergent theories in physics, biology, and beyond. J. Chem. Phys. 143(1):010901.
[39]. Brown KS, HillCC, Calero GA, Myers CR, Lee KH, Sethna JP, Cerione RA (2005) The statistical mechanics of complex signaling networks: nerve growth factor signaling. Phys. Biol. 1:184-195.
[40]. Lee Y, Chen PW and Voit EO (2011) Analysis of operating principles with S-system models. Math. Biosci. 231:49-60.
[41]. Wu SJ, Lin CT (2000) Optimal fuzzy controller design: local concept approach. IEEE Trans. Fuzzy Syst. 8(2):171-185.
[42]. Wu SJ (2008) Reply to “Further comment on “optimal fuzzy controller design: local concept approach””. IEEE Trans. Fuzzy Syst. 16(2):547-549.
[43]. Tsai KY, Wang FS (2005) Evolutionary optimization with data collocation for reverse engineering of biological network. Bioinformatics 21:1180-1188.
[44]. Gonzalez OR, Küper C, Jung K, Naval-JrPC, Mendoza E (2007) Parameter estimation using simulated annealing for S-system

models of biochemical networks. Bioinformatics 23:480–486.
[45]. Hlavacek WS, Savageau MA (1996) Rules for coupled expression of regulator and effector genes in inducible circuits. J Mol Biol 255:121–139.
[46]. NomanN, Iba H (2006) Inference of genetic networks using S-system: information criteria for model selection. in 2006 GECCO: Proc Conf Genetic Evolutionary Comput 263-270.
[47]. Kimura S, Ide K, Kashihara A, Kano M, Mariko H, Masui R, Nakagawa N, Yokoyama S, Kuramitsu S, Konagaya A (2005) Inference of S-system models of genetic networks using a cooperative coevolutionary algorithm. Bioinformatics 21:1154–1163.
[48]. Ohtake H, Tanaka K, Wang HO (2001) Fuzzy modeling via sector nonlinearity concept. Proceedings Joint 9th IFSA World Congress and 20th NAFIPS International Conference (Cat. No. 01TH8569), Vancouver, BC, Canada, 127-132.
[49]. Wu SJ, Chen WY, Chou CH, Wu CT (2013) Prototype of integrated pseudo-dynamic crosstalk network for cancer molecular mechanism. Math. Biosci. 243(1):81-98.
[50]. Wu SJ, Wu CT and Chang YC (2008) Neural–fuzzy gap control for a current/voltage-controlled 1/4-vehicle MagLev system. IEEE Trans. Intell. Transp. Syst. 9(1):122-136.
[51]. Wu SJ, Chiang HH, Chen CJ, WuBF, Perng JW, Lee TT (2008) The heterogeneous systems integration design and implementation for lane keeping on a vehicle. IEEE Trans. Intell. Transp. Syst. 9(2): 246-263.

Supplement materials

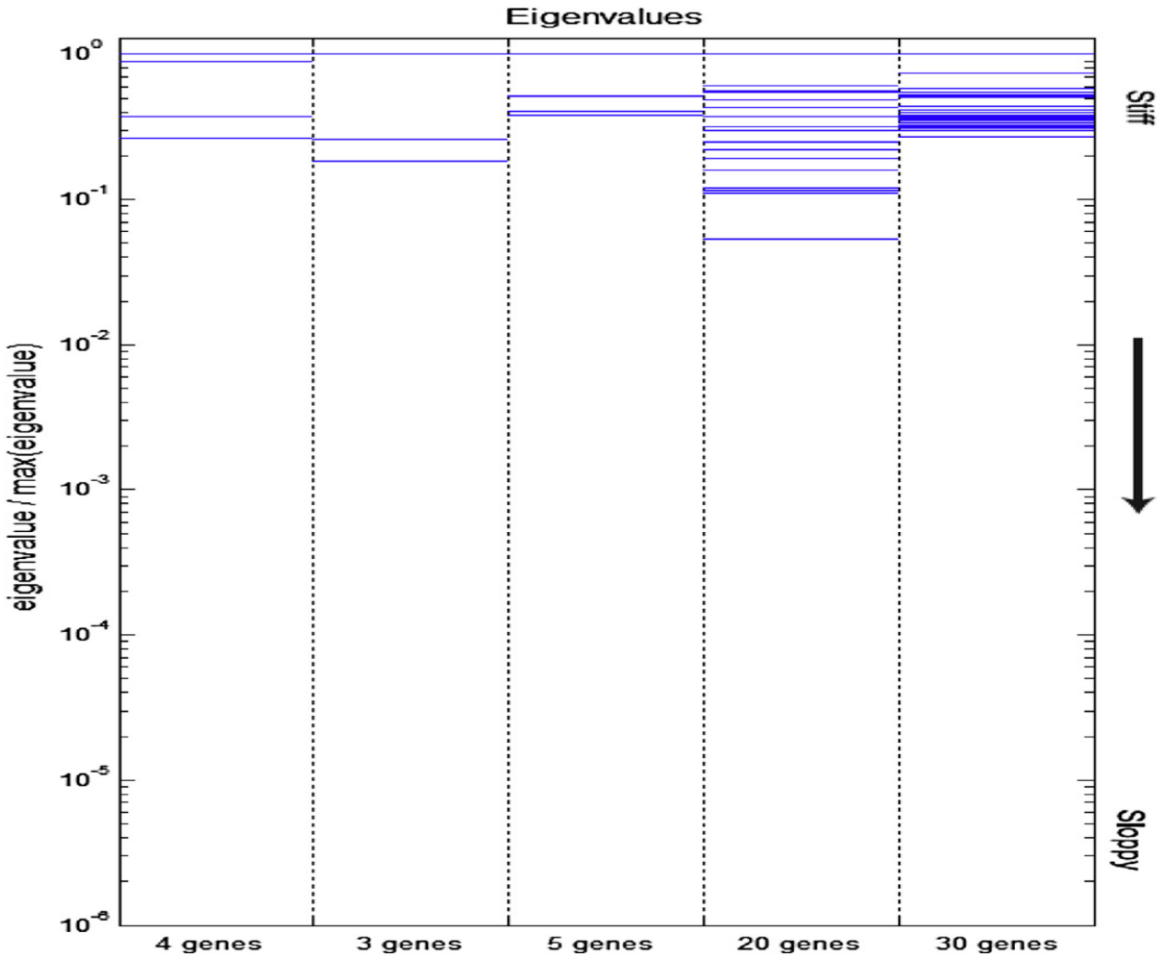

Figure S1: Sloppiness spectrum ***near steady state***of S-Systems [15]

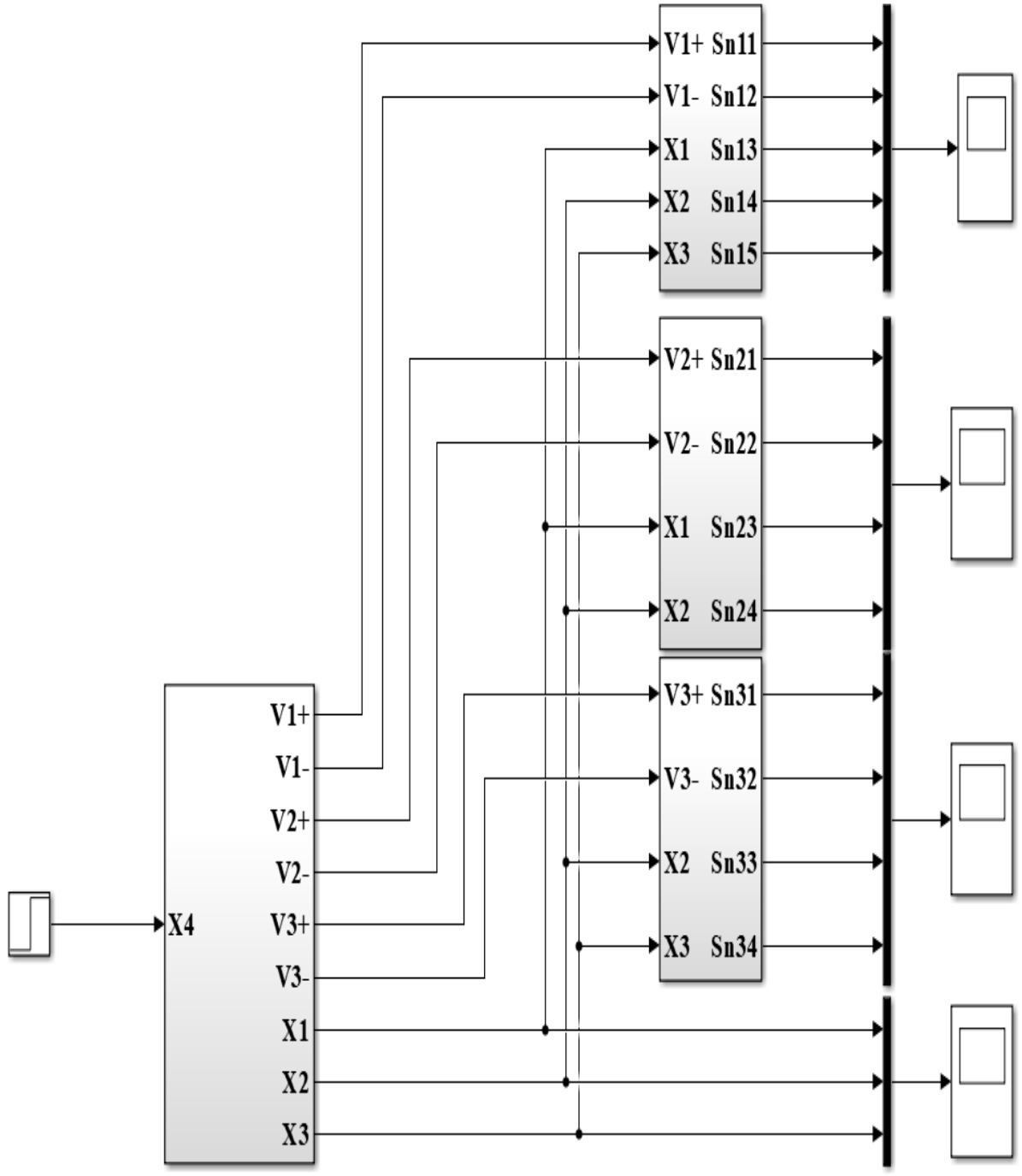

Figure S2: Block diagram for ***dynamic densitivity*** of the three-tier cascade pathway S-Systems [24]

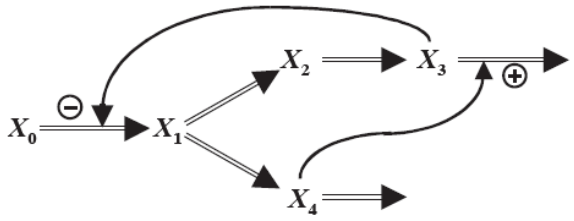

$$\dot{x}_1 = \alpha_1 x_3^{g_{13}} x_0^{g_{10}} - \beta_1 x_1^{h_{11}},$$
$$\dot{x}_2 = \alpha_2 x_1^{g_{21}} - \beta_2 x_2^{h_{22}},$$
$$\dot{x}_3 = \alpha_3 x_2^{g_{32}} - \beta_3 x_3^{h_{33}} x_4^{h_{34}},$$
$$\dot{x}_4 = \alpha_4 x_1^{g_{41}} - \beta_4 x_4^{h_{44}}.$$

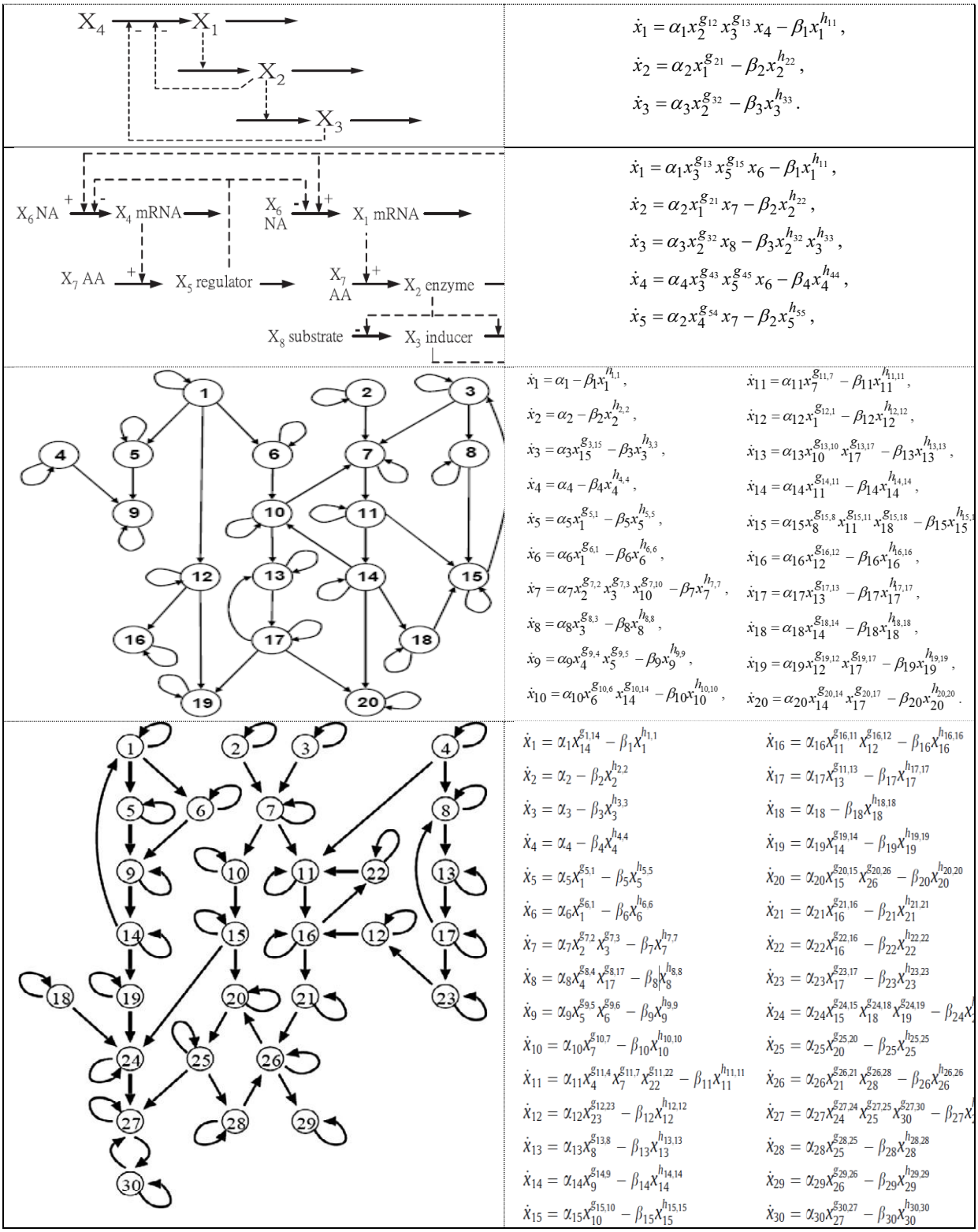

$$\dot{x}_1 = \alpha_1 x_2^{g_{12}} x_3^{g_{13}} x_4 - \beta_1 x_1^{h_{11}},$$
$$\dot{x}_2 = \alpha_2 x_1^{g_{21}} - \beta_2 x_2^{h_{22}},$$
$$\dot{x}_3 = \alpha_3 x_2^{g_{32}} - \beta_3 x_3^{h_{33}}.$$

$$\dot{x}_1 = \alpha_1 x_3^{g_{13}} x_5^{g_{15}} x_6 - \beta_1 x_1^{h_{11}},$$
$$\dot{x}_2 = \alpha_2 x_1^{g_{21}} x_7 - \beta_2 x_2^{h_{22}},$$
$$\dot{x}_3 = \alpha_3 x_2^{g_{32}} x_8 - \beta_3 x_2^{h_{32}} x_3^{h_{33}},$$
$$\dot{x}_4 = \alpha_4 x_3^{g_{43}} x_5^{g_{45}} x_6 - \beta_4 x_4^{h_{44}},$$
$$\dot{x}_5 = \alpha_2 x_4^{g_{54}} x_7 - \beta_2 x_5^{h_{55}},$$

$$\dot{x}_1 = \alpha_1 - \beta_1 x_1^{h_{1,1}},$$
$$\dot{x}_2 = \alpha_2 - \beta_2 x_2^{h_{2,2}},$$
$$\dot{x}_3 = \alpha_3 x_{15}^{g_{3,15}} - \beta_3 x_3^{h_{3,3}},$$
$$\dot{x}_4 = \alpha_4 - \beta_4 x_4^{h_{4,4}},$$
$$\dot{x}_5 = \alpha_5 x_1^{g_{5,1}} - \beta_5 x_5^{h_{5,5}},$$
$$\dot{x}_6 = \alpha_6 x_1^{g_{6,1}} - \beta_6 x_6^{h_{6,6}},$$
$$\dot{x}_7 = \alpha_7 x_2^{g_{7,2}} x_3^{g_{7,3}} x_{10}^{g_{7,10}} - \beta_7 x_7^{h_{7,7}},$$
$$\dot{x}_8 = \alpha_8 x_3^{g_{8,3}} - \beta_8 x_8^{h_{8,8}},$$
$$\dot{x}_9 = \alpha_9 x_4^{g_{9,4}} x_5^{g_{9,5}} - \beta_9 x_9^{h_{9,9}},$$
$$\dot{x}_{10} = \alpha_{10} x_6^{g_{10,6}} x_{14}^{g_{10,14}} - \beta_{10} x_{10}^{h_{10,10}},$$
$$\dot{x}_{11} = \alpha_{11} x_7^{g_{11,7}} - \beta_{11} x_{11}^{h_{11,11}},$$
$$\dot{x}_{12} = \alpha_{12} x_1^{g_{12,1}} - \beta_{12} x_{12}^{h_{12,12}},$$
$$\dot{x}_{13} = \alpha_{13} x_{10}^{g_{13,10}} x_{17}^{g_{13,17}} - \beta_{13} x_{13}^{h_{13,13}},$$
$$\dot{x}_{14} = \alpha_{14} x_{11}^{g_{14,11}} - \beta_{14} x_{14}^{h_{14,14}},$$
$$\dot{x}_{15} = \alpha_{15} x_8^{g_{15,8}} x_{11}^{g_{15,11}} x_{18}^{g_{15,18}} - \beta_{15} x_{15}^{h_{15,}}$$
$$\dot{x}_{16} = \alpha_{16} x_{12}^{g_{16,12}} - \beta_{16} x_{16}^{h_{16,16}},$$
$$\dot{x}_{17} = \alpha_{17} x_{13}^{g_{17,13}} - \beta_{17} x_{17}^{h_{17,17}},$$
$$\dot{x}_{18} = \alpha_{18} x_{14}^{g_{18,14}} - \beta_{18} x_{18}^{h_{18,18}},$$
$$\dot{x}_{19} = \alpha_{19} x_{12}^{g_{19,12}} x_{17}^{g_{19,17}} - \beta_{19} x_{19}^{h_{19,19}},$$
$$\dot{x}_{20} = \alpha_{20} x_{14}^{g_{20,14}} x_{17}^{g_{20,17}} - \beta_{20} x_{20}^{h_{20,20}}.$$

$$\dot{X}_1 = \alpha_1 X_{14}^{g_{1,14}} - \beta_1 X_1^{h_{1,1}}$$
$$\dot{X}_2 = \alpha_2 - \beta_2 X_2^{h_{2,2}}$$
$$\dot{X}_3 = \alpha_3 - \beta_3 X_3^{h_{3,3}}$$
$$\dot{X}_4 = \alpha_4 - \beta_4 X_4^{h_{4,4}}$$
$$\dot{X}_5 = \alpha_5 X_1^{g_{5,1}} - \beta_5 X_5^{h_{5,5}}$$
$$\dot{X}_6 = \alpha_6 X_1^{g_{6,1}} - \beta_6 X_6^{h_{6,6}}$$
$$\dot{X}_7 = \alpha_7 X_2^{g_{7,2}} X_3^{g_{7,3}} - \beta_7 X_7^{h_{7,7}}$$
$$\dot{X}_8 = \alpha_8 X_4^{g_{8,4}} X_{17}^{g_{8,17}} - \beta_8 X_8^{h_{8,8}}$$
$$\dot{X}_9 = \alpha_9 X_5^{g_{9,5}} X_6^{g_{9,6}} - \beta_9 X_9^{h_{9,9}}$$
$$\dot{X}_{10} = \alpha_{10} X_7^{g_{10,7}} - \beta_{10} X_{10}^{h_{10,10}}$$
$$\dot{X}_{11} = \alpha_{11} X_4^{g_{11,4}} X_7^{g_{11,7}} X_{22}^{g_{11,22}} - \beta_{11} X_{11}^{h_{11,11}}$$
$$\dot{X}_{12} = \alpha_{12} X_{23}^{g_{12,23}} - \beta_{12} X_{12}^{h_{12,12}}$$
$$\dot{X}_{13} = \alpha_{13} X_8^{g_{13,8}} - \beta_{13} X_{13}^{h_{13,13}}$$
$$\dot{X}_{14} = \alpha_{14} X_9^{g_{14,9}} - \beta_{14} X_{14}^{h_{14,14}}$$
$$\dot{X}_{15} = \alpha_{15} X_{10}^{g_{15,10}} - \beta_{15} X_{15}^{h_{15,15}}$$
$$\dot{X}_{16} = \alpha_{16} X_{11}^{g_{16,11}} X_{12}^{g_{16,12}} - \beta_{16} X_{16}^{h_{16,16}}$$
$$\dot{X}_{17} = \alpha_{17} X_{13}^{g_{11,13}} - \beta_{17} X_{17}^{h_{17,17}}$$
$$\dot{X}_{18} = \alpha_{18} - \beta_{18} X_{18}^{h_{18,18}}$$
$$\dot{X}_{19} = \alpha_{19} X_{14}^{g_{19,14}} - \beta_{19} X_{19}^{h_{19,19}}$$
$$\dot{X}_{20} = \alpha_{20} X_{15}^{g_{20,15}} X_{26}^{g_{20,26}} - \beta_{20} X_{20}^{h_{20,20}}$$
$$\dot{X}_{21} = \alpha_{21} X_{16}^{g_{21,16}} - \beta_{21} X_{21}^{h_{21,21}}$$
$$\dot{X}_{22} = \alpha_{22} X_{16}^{g_{22,16}} - \beta_{22} X_{22}^{h_{22,22}}$$
$$\dot{X}_{23} = \alpha_{23} X_{17}^{g_{23,17}} - \beta_{23} X_{23}^{h_{23,23}}$$
$$\dot{X}_{24} = \alpha_{24} X_{15}^{g_{24,15}} X_{18}^{g_{24,18}} X_{19}^{g_{24,19}} - \beta_{24} X_{}^{}$$
$$\dot{X}_{25} = \alpha_{25} X_{20}^{g_{25,20}} - \beta_{25} X_{25}^{h_{25,25}}$$
$$\dot{X}_{26} = \alpha_{26} X_{21}^{g_{26,21}} X_{28}^{g_{26,28}} - \beta_{26} X_{26}^{h_{26,26}}$$
$$\dot{X}_{27} = \alpha_{27} X_{24}^{g_{27,24}} X_{25}^{g_{27,25}} X_{30}^{g_{27,30}} - \beta_{27} X_{}^{}$$
$$\dot{X}_{28} = \alpha_{28} X_{25}^{g_{28,25}} - \beta_{28} X_{28}^{h_{28,28}}$$
$$\dot{X}_{29} = \alpha_{29} X_{26}^{g_{29,26}} - \beta_{29} X_{29}^{h_{29,29}}$$
$$\dot{X}_{30} = \alpha_{30} X_{27}^{g_{30,27}} - \beta_{30} X_{30}^{h_{30,30}}$$

Figure S3: Biological systems and related S-system representations for validating S-system sloppiness. The parameter values are cited from [43-47].